

Analytical Treatment of Large Leak  
Pressure Behavior in LMFBR Steam Generators

July 1980

複製又はこの資料の入手については、下記にお問い合わせ下さい。

〒311-13 茨城県東茨城郡大洗町成田町4002

動力炉・核燃料開発事業団 大洗工学センター

システム開発推進部 技術管理室

Inquiries about copyright and reproduction should be addressed to:  
Technology Management Section, O-arai Engineering Center, Power Reactor  
and Nuclear Fuel Development Corporation 4002, Narita O-arai-machi Higashi-  
Ibaraki-gun, Ibaraki, 311-14, Japan

動力炉・核燃料開発事業団 (Power Reactor and Nuclear Fuel Development  
Corporation)

Analytical Treatment of Large Leak  
Pressure Behavior in LMFBR Steam Generators

Masao Hori\* and Osamu Miyake\*

Abstract

Simplified analytical methods applicable to the estimation of initial pressure spike in case of a large leak accident in LMFBR steam generators were devised as follows ;

- (i) Estimation of the initial water leak rate by the centered rarefaction wave method,
- (ii) Estimation of the initial pressure spike by the one-dimensional compressible method with either the columnar bubble growth model or the spherical bubble growth model.

These methods were compared with relevant experimental data or other more elaborate analyses and validated to be usable in simple geometry and limited time span cases.

Application of these methods to an actual steam generator case was explained and demonstrated.

---

\* Steam Generator Division, O-arai Engineering Center, PNC.

## CONTENTS

	Page
I. Introduction -----	1
II. Estimation of Initial Water Leak Rate -----	2
III. Initial Pressure Spike Calculation by One-dimensional Compressible Model -----	6
Columnar Bubble Growth Model -----	6
Spherical Bubble Growth Model -----	8
Comparison of Columnar and Spherical Bubble Growth Model -----	11
IV. Application to the Pressure Spike Evaluation -----	12
V. Concluding Remarks -----	14
Reference -----	15

## LIST OF FIGURES

		Page
Fig. 1	Pressure Transient Inside Tube Filled with Stationary Pressurized Liquid following Rupture at One End (Propagation of Centered Rarefaction Wave) .	16
Fig. 2	Calculation Example of Initial Leak Rate for the Standard Problem Condition.	17
Fig. 3	Water/Steam Condition along Heat Transfer Tube of Helical Type Steam Generator (Evaporator) of 200 MWt Class.	18
Fig. 4	Initial Water Leak Rate for 1 DEG Rupture of Helical-coil, Once-through Steam Generator.	19
Fig. 5	Steady-state Water Leak Rate for 1 DEG Rupture of Helical-coil, Once-through Steam Generator.	20
Fig. 6	One-dimensional Compressible Models.	21
Fig. 7	Prediction of Spike Pressure by One-dimensional Compressible Model ( Columnar Bubble Growth)	22
Fig. 8	Prediction of Initial Pressure Spike by Columnar Bubble, One-dimensional Compressible Model-Comparison with Experimental Data of SWAT-1 Tests (PNC)	23
Fig. 9	Schematic Configuration of Helical Coil Type Steam Generator (Evaporator) of 200 MWt Class.	24

LIST OF FIGURES (Cont'd)

		Page
Fig. 10	Typical Pressure Transient of 1 DEG Rupture Calculated by Spherical Bubble One-dimensional Compressible Model (SP-AX Code). -----	25
Fig. 11	Comparison of Spherical Compressible (SWACS) and Spherical Incompressible (SP-AX) models. -----	26
Fig. 12	Comparison of Columnar and Spherical Bubble Growth Models -----	27
Fig. 13	Initial Leak Rate vs. Water/Steam Pressure and Enthalpy. -----	28

Analytical Treatment of Large Leak  
Pressure Behavior in LMFBR Steam Generators

I. Introduction

In the design of steam generator systems for LMFBR plants, large leak sodium-water reactions have been taken into consideration. A moment after the beginning of the water leak into sodium, there is a high pressure pulse which is usually termed "initial pressure spike". The value of this pressure spike depends on the initial water leak rate and the acoustic constraint characteristics of the sodium flow path inside the steam generator. A secondary peak pressure, which is termed "quasi-steady pressure", occurs after the rupture disc bursts, and its early value depends on the inertia constraint characteristics in the pressure relief system, while its asymptotic value depends on the resistance constraint characteristics in the pressure relief system.

Computer codes to analyze the pressure transients caused by large-leak sodium-water reactions in a steam generator, and its related systems have been developed in various countries, and used for the detailed analysis of large-leak pressure behavior in LMFBR steam generators.

On the other hand, simplified analytical treatment is convenient for the purpose of identifying general behavior trends, performing parametric studies, and for verifying computer code calculations. However, analytical treatment is possible only for simple geometries and limited time spans.

In this report, simplified analytical methods applicable to the large-leak initial pressure spike behavior are described.

## II. Estimation of Initial Water Leak Rate

An equation to calculate the water leak rate immediately following the rupture of a heat-transfer tube of steam generators can be derived by assuming the following conditions :

- (i) Thermodynamic equilibrium between water and steam phases,
- (ii) Uniform enthalpy profile along the heat-transfer tube, and
- (iii) No frictional pressure losses.

As shown in Fig. 1, if a rupture occurs at the end of tube filled with stationary water (or water/steam mixture), a rarefaction wave is created which travels along the tube.

If the outside pressure,  $P_o$ , is higher than the saturation pressure of water,  $P_{sat}$ , in the pipe, no phase change occurs, and the initial flow velocity,  $u$ , can be obtained by Eq. (1).

$$u = g_c \frac{P_1 - P_o}{c \rho} \quad (1)$$

where  $c$  is the sonic velocity of water,  $\rho$  the density of water,  $P_1$  the initial pressure of water, and  $g_c$  the gravity conversion factor.

If, however, the outside pressure is lower than the saturation pressure, a phase change occurs by the depressurization when the tube is ruptured. The propagation of the rarefaction wave is shown in Fig. 1, where a series of the centered rarefaction waves, corresponding to different pressures, are shown in the time-distance plane. The differential velocity change due to the pressure change may be expressed as follows :

$$du = -g_c \frac{dp}{\rho c} \quad (2)$$



where  $u$  and  $\rho$  are the velocity and density of the fluid, respectively. The initial velocity of fluid,  $u_o$ , flowing out from the ruptured end to the outside static fluid with pressure  $P_o$ , can be expressed by Eq. (3) :

$$u_o = -g_c \int_{P_1}^{P_o} \frac{dp}{\rho c} \quad (3)$$

In performing the integration, if the condition of  $u \geq c$  is reached, that is the critical flow condition, then the velocity is expressed by the following equation.

$$u_c = -g_c \int_{P_1}^{P_c} \frac{dp}{\rho c} \quad (4)$$

where  $P_c$  is the pressure at the condition of  $u = c$ .

The initial mass flow rate just after the rupture of a tube can be calculated for sub-critical flow and critical flow by the following equations.

If  $u < c$ , in the course of pressure change from  $P_1$  to  $P_o$  (sub-critical discharge) :

$$G = A \rho_o u_o = -A \rho_o g_c \int_{P_1}^{P_o} \frac{dp}{\rho c} \quad (5)$$

If  $u \geq c$ , in the course of pressure change from  $P_1$  to  $P_o$  (critical discharge) ;

$$G = A \rho_c u_c = -A \rho_c g_c \int_{P_1}^{P_c} \frac{dp}{\rho c} \quad (6)$$

where  $A$  is the cross-sectional area of the tube. Most of the leak conditions encountered in steam generators are those of critical flow discharge.

To calculate the flow rate numerically using Eq. (5) or (6), an isentropic process may be assumed to obtain the quality of water/steam mixture from the initial conditions. Furthermore, homogeneous flow (no slip between water and steam phase) may be assumed for determining the density of water/steam mixture from the quality.

As an example of the calculations, Fig. 2 shows results for a problem of a discharge of initially stagnant pressurized water ( $225^{\circ}\text{C}$ ,  $71.32\text{ kg/cm}^2\text{ abs}$ ) from a 73 mm inner diameter tube to the atmosphere. This problem is identical to one of the conditions in the Edwards-O'Brien experiment<sup>(1)</sup>, and has been selected by CSNI as an International Standard Problem. As shown in Fig. 2, the critical flow condition is reached at pressure of  $19.1\text{ kg/cm}^2\text{ abs}$ , and at a mass flow rate of  $45.2\text{ kg/sec}$ . The mass flow rate obtained is the initial value, but under the simplifying assumptions of this analysis, this flow rate continues until the reflected wave from the tube end returns back to the ruptured end.

Next, an example of the application of this calculational method (Centered Rarefaction Method or CRW method) to a steam generator is shown. The initial water leak rate from a double-ended guillotine rupture of the heat-transfer tube in a once-through, helical-coil type steam generator (evaporator of 200 MWt class) is calculated. The tube diameter is 19 mm inner diameter and the tube length is 61.15 m. Water condition at inlet header is  $154.2\text{ kg/cm}^2\text{ abs}$  and  $240^{\circ}\text{C}$ ; steam condition at outlet header is  $145.7\text{ kg/cm}^2\text{ abs}$  and  $369^{\circ}\text{C}$ . The water/steam condition along the heat transfer tube is shown in Fig. 3. The initial water leak rates along the tube length are calculated and shown in Fig. 4, assuming the outside pressure is below the critical pressure,  $P_c$ . As there is flow in the heat-transfer tube, the leak rates from the upstream

and downstream ends differ. The initial leak rate becomes maximum when the rupture occurs at the saturated water condition. The relation between the initial leak rate and the position of leak (Fig. 4) is very much different from the relation between the steady-state leak rate and the position of leak (Fig. 5) which is calculated for the same condition by the homogeneous equilibrium model.

The calculated initial leak rate can be used for the determination of the initial pressure spike, because the leak rate does not change significantly until the reflected wave returns back to the ruptured ends, and this wave-returning time is usually longer than the duration of initial pressure spike.

### III. Initial Pressure Spike Calculation by One-dimensional Compressible Model

The time span of initial pressure transient is the length of time in which the initial pressure wave travels between the top (or the sodium free surface) and the bottom of steam generator two or three times. In the case of cover-gas type steam generators, the duration or width of the initial pressure spike is considered to be equal to the time it takes the pressure wave to reflect back from the free surface. In a unit-type steam generator of 200 MWt class (sodium level = 10 m high), the duration of the initial pressure spike is about 10 msec for the leak position of maximum leak rate (the saturated water condition). Simplified analysis of the initial pressure spike can be made using the one-dimensional model for the time span of around 10 msec during which the water leak rate is considered to be nearly constant at the initial value.

#### Columnar Bubble Growth Model

If the hydrogen gas bubble growth in the steam generator is modelled as columnar bubble growth in an acoustically infinite, one-dimensional compressible liquid channels, as shown in Fig. 6 (a), then the velocity of the gas-liquid interface,  $u_L$ , is expressed by Eq. (7). The gravitational force and the frictional pressure drop in this analysis are neglected.

$$u_L = \frac{P_B - P_O}{\rho_L c} \quad (7)$$

$P_O$  : Pressure of liquid at reset

$P_B$  : Pressure of gas

$\rho_L$  : Density of liquid

$c$  : Sonic velocity of liquid

From the equation of state of an ideal gas,

$$P_B = \frac{MRT}{V} \quad (8)$$

M : Mass of gas

R : Gas constant

T : Absolute temperature of gas

V : Volume of gas

The liquid is pushed away in both upward and downward directions, then

$$u_L = \frac{\dot{V}}{2A} \quad (9)$$

A : Cross-sectional area of channel in one direction

From Eqs. (7), (8) (9), the following equations are derived;

$$\frac{P_B - P_O}{\rho_L c} = \frac{1}{2A} \frac{RT}{P_B} \dot{M} \quad (10)$$

$\dot{M}$  : Increase rate of mass of gas

Solving Eq. (10) for  $P_B$ ,

$$\frac{P_B}{P_O} = \frac{1}{2} \left( 1 + \sqrt{1 + \frac{4 \rho_L c R T \dot{M}}{2 A P_O^2}} \right) \quad (11)$$

In Eq. (11),  $(P_B/P_O)$  is the dimensionless ratio of the pressure spike to the pressure at rest, and  $(4 \rho_L c R T \dot{M} / 2 A P_O^2)$  is a dimensionless number used to determine the magnitude of pressure spike, which is denoted by  $N_{sp}$  or Spike number. In Fig. 7 this relation is shown graphically. In Fig. 7, the predicted Spike number for the 1 DEG leak case of the steam generator (Fig. 9), and the range of Spike number of PNC's SWAT-1 and SWAT-3 tests are shown. For the case of one-directional bubble growth, such as the sodium-

water reaction at a dead-end (most of the SWAT-1 test were this case), A is used instead of 2A in Eq. (11).

The increase rate of hydrogen  $\dot{M}$ , is substituted by the water leak rate, G.

$$\dot{M} = fG/9 \quad (12)$$

f : Mol conversion ratio of  $H_2/H_2O$

Then, the initial pressure spike for two directional bubble growth is expressed by Eq. (13).

$$P_B = \frac{P_O}{2} \left( 1 + \sqrt{1 + \frac{4 \rho_L cRTf}{18AP_O^2} \cdot G} \right) \quad (13)$$

For one directional bubble growth, a value of the constant equal to 9 should be used instead of 18 in Eq. (13).

Comparison of the pressure predicted by Eq. (13) with the experimental data<sup>(2)</sup> from the SWAT-1 test rig is shown in Fig. 8.

These tests were run with various water and sodium conditions which are designated by the test series in Fig. 8. The absolute temperature of hydrogen gas (T), and the conversion ratio (f) are the values to be determined from experiments. The combination of  $T = 1273 \text{ }^\circ\text{K}$  and  $f = 0.65 \text{ mol H/mol } H_2O$  gives a fairly good agreement between the experimental and predicted values.

#### Spherical Bubble Growth Model

The bubble growth in the steam generator can be analyzed using a combined model which assumes : 1) spherical bubble growth in an incompressible liquid in the vicinity of the reaction source, and 2) a one-dimensional (axial) motion

model in a compressible liquid away from the reaction source. This analysis model is shown in Fig. 6 (b). This combined model is more realistic than the single columnar bubble model (Fig. 6 (a)) because it takes into consideration the spherical growth effect of the bubble. Although a three-dimensional, compressible model would be more accurate, this spherical bubble growth model provides acceptable results with much less analytic complexity. The model is a realistic approximation because in the time span of the initial pressure spike, the pressure wave bounces many times between the bubble and the wall of the fluid containment, and it can be reasonably treated as growth in an incompressible liquid, except at the initial moment.

For  $r_B \ll r'$ , Rayleigh's equation can be applied to the bubble growth,

$$\dot{u}_B = \frac{P_B - P'}{\rho_L r_B} - \frac{3}{2} \frac{u_B}{r_B} \quad (14)$$

$r_B$  : Radius of bubble

$r'$  : Equivalent radius of channel

$P'$  : Liquid pressure near channel wall

$u_B$  : Radial velocity of gas-liquid interface

The axial motion of liquid is constrained acoustically, then

$$\dot{u}_L = \frac{\dot{p}'}{\rho_L c} \quad (15)$$

$u_L$  : Axial velocity of liquid in upward and downward direction.

From the volume balance for the two directions (up and down)

$$2Au_L = 4\pi r_B^2 u_B \quad (16)$$

Equations (14), (15) and (16) can be solved numerically (SP-AX code) to yield the bubble pressure ( $P_B$ ) and the liquid pressure near bubble ( $P'$ ), which corresponds to the spike pressure.

As an example of this calculation method (SP-AX code), the spike pressure is calculated for a water leak in a helical-coil type steam generator (evaporator) of 200 MWt class (Fig. 9). The results of calculation for a stepwise leak rate of 12 kg/sec is shown in Fig. 10. The maximum sodium pressure (spike pressure) was calculated to be  $15.5 \text{ kg/cm}^2$  at 2.4 msec using the spherical bubble growth model, while the spike pressure from the columnar bubble growth model (Eq. (13)) using the same condition is  $12.3 \text{ kg/cm}^2$ .

Next, the results of this calculation model are compared with those by SWACS code<sup>(3)</sup> which uses more elaborate calculation model, thus we can verify the adequacy of the simplified spherical bubble growth model (SP-AX code calculation). The calculations are made for the configuration shown in Fig. 9. The comparison is shown in Fig. 11. Both results coincide quite well.

The SWACS code assumes the compressible-sphere, compressible-cylinder model, while the SP-AX code assumes the incompressible-sphere, compressible-cylinder model. As mentioned above, for the time span considered, the bubble growth under the constraint of wall can be approximated by that in incompressible media. Therefore, it is considered natural that both models give almost similar results. Small discrepancies in Fig. 11 between the two models are due to the different positions for pressure calculation and to the reflection wave from the lower plenum which SWACS does and SP-AX does not take into consideration.

From these bench-mark calculations, it is concluded that the spherical bubble growth model (incompressible sphere, compressible cylinder model) is a reasonably accurate method of estimating the initial pressure spike with



much less analytic complexity than the more elaborate calculation method.

#### Comparison of Columnar and Spherical Bubble Growth Models

Results of comparison calculation between the columnar bubble growth model and the spherical bubble growth model are shown in Fig. 12. These calculations are made with three different leak rates on the helical coil type steam generator of 200 MWt class of which dimensions are given in Fig. 9.

The pressure-time histories for the cases of 6 and 24 kg/sec leak rate are similar to that in Fig. 10 which is the case of 12 kg/sec leak rate. In Fig. 12, the maximum pressure and the pressure at 10 msec both calculated by the SP-AX codes, and calculated by Eq. (13) are compared. All these pressures are proportional to about 0.46 power of the leak rate, of which relation can be deduced from Eq. (13). The pressure at 10 msec (almost steady value) calculated by the SP-AX code is almost the same as the pressure calculated by Eq. (13), while the maximum pressure calculated by the SP-AX code is about 25% higher than the pressure calculated by Eq. (13).

From these comparisons, it can be said that the spike pressure can be estimated by the simple model of the columnar bubble growth, to be more accurate, with the correction factor of 1.25.

The spherical bubble growth model usually gives higher, and more accurate, pressure values than the columnar bubble growth model; therefore from Fig. 8 it can be said that the assumption of  $f \times T = 0.65 \times 1273$  can be used as pessimistic input values (25% overestimate) for initial pressure spike analysis with the spherical bubble growth model.

#### IV. Application to the Pressure Spike Evaluation

The simplified analytical treatment so far explained can be applied to the actual steam generator for the purpose of quick and easy estimation of the pressure spike.

The procedure is as follows ;

- (i) Calculate the initial leak rate,  $G$ , by the CRW method using Eq. (6). (cf Fig. 4). For convenience sake, the leak rates per unit cross sectional area of tube are calculated for various pressures and enthalpies, and shown graphically in Fig. 13.
- (ii) Calculate the spike pressure,  $P_B$ , by Eq. (13). Appropriate values of  $f$  and  $T$  should be used.
- (iii) The maximum spike pressure would be  $P_B \times 1.25$
- (iv) Calculate the duration of initial pressure spike,  $t_{sp}$ , by  $\left\{ \begin{array}{l} \text{(Depth of} \\ \text{leak position under the free surface)} \times 2 / \text{(Sonic velocity of sodium)} \end{array} \right\}$   
(Cover gas type steam generator only)

An example of calculation is shown for 1 DEG (Double-ended guillotine) rupture at the saturated water position of the steam generator shown in Fig. 9, and Fig. 3 which follows ;

- (i) Initial leak rate,  $G$

From Fig. 4

$$G = 16.5 \text{ kg/sec}$$

(ii) Spike pressure,  $P_B$

From Eq. (13), assuming  $f \times T = 0.65 \times 1273$

$$P_B = 14.2 \text{ kg/cm}^2$$

(iii) Maximum spike pressure,  $P_B, \text{max.}$

$$P_{B, \text{max}} = 14.2 \times 1.25 = 18 \text{ kg/cm}^2$$

(iv) Duration of initial pressure spike,  $t_{sp}$

$$\text{Depth} = 5.375 \text{ m}$$

$$\text{Sonic Velocity} = 1307.9 \text{ m/sec}$$

$$t_{sp} = 8.2 \text{ (msec)}$$

## V. Concluding Remarks

Simplified analytical methods applicable to the estimation of initial pressure spike in case of a large leak accident in LMFBR steam generators were devised as follows ;

- (i) Estimation of the initial water leak rate by the centered rarefaction wave method, and
- (ii) Estimation of the initial pressure spike by the one-dimensional compressible method with either the columnar bubble growth model or the spherical bubble growth model.

These methods were compared with relevant experimental data or other more elaborate analyses and validated to be usable in simple geometry and limited time span cases.

Application of these methods to an actual steam generator case was explained and demonstrated.

These simplified methods are considered to be convenient for the purpose of making rough estimation, identifying general trends, performing parametric studies, and in some cases, verifying computer code calculations, of the initial pressure spike.

[References]

- (1) Edwards, A. R., et al., "Studies of Phenomena Connected with the Depressurization of Water Reactors", J. British Nuc. Energy Soc., 9, 125-135 (1970)
- (2) Sato, M., et al., "Initial Pressure Spike and Its Propagation in Sodium-Water Reaction Tests for MONJU Steam Generators", 4th International Conference on Structural Mechanics in Reactor Technology, San Francisco, (Aug., 1977).
- (3) Hori, M., et al., "Safety Evaluation of the MONJU Steam Generator", International Meeting on Fast Reactor Safety and Related Physics, Chicago, (Oct., 1976).

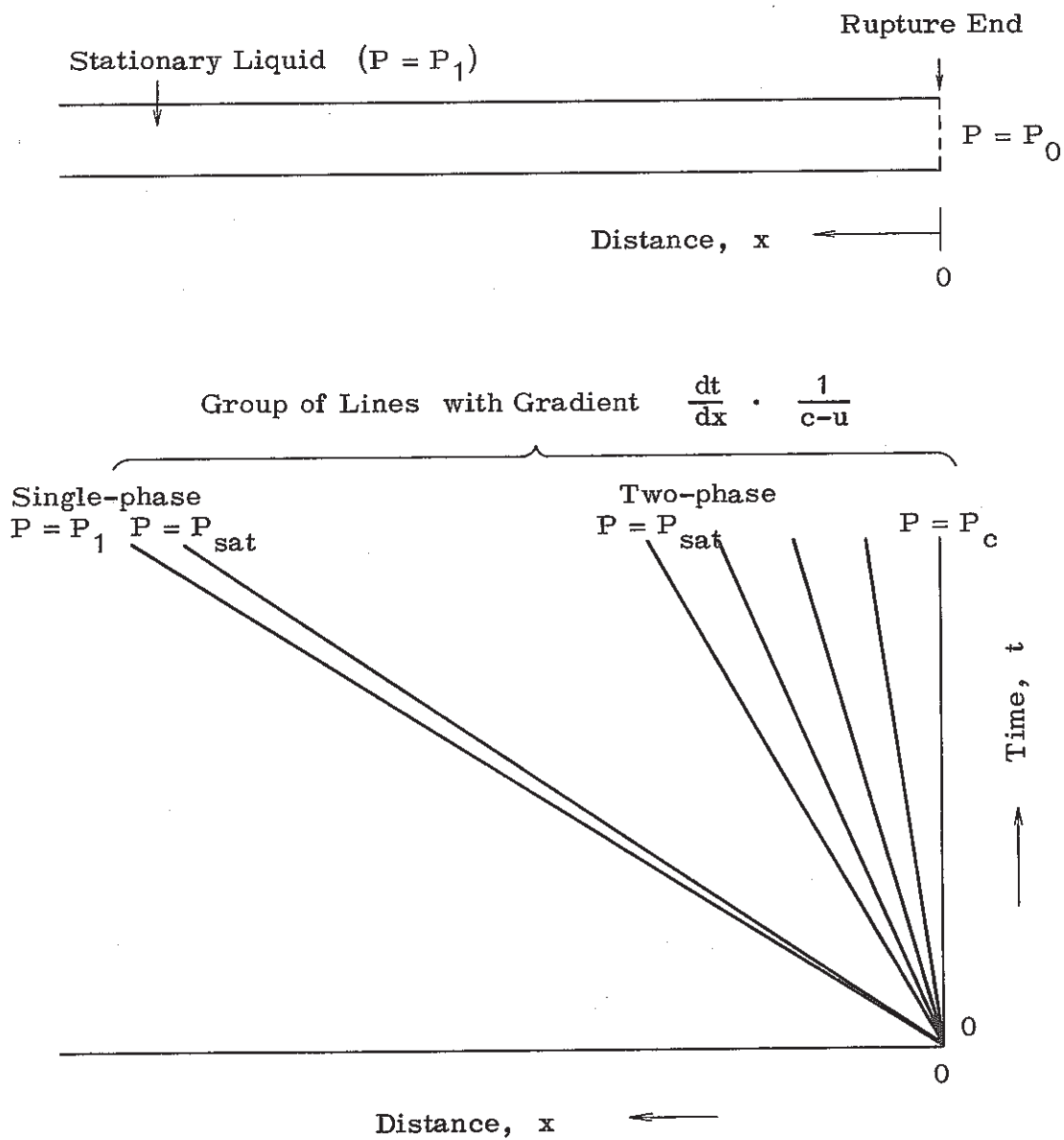


Fig. 1 Pressure Transient inside Tube Filled with Stationary Pressurized Liquid following Rupture at One End (Propagation of Centered Rarefaction Wave)

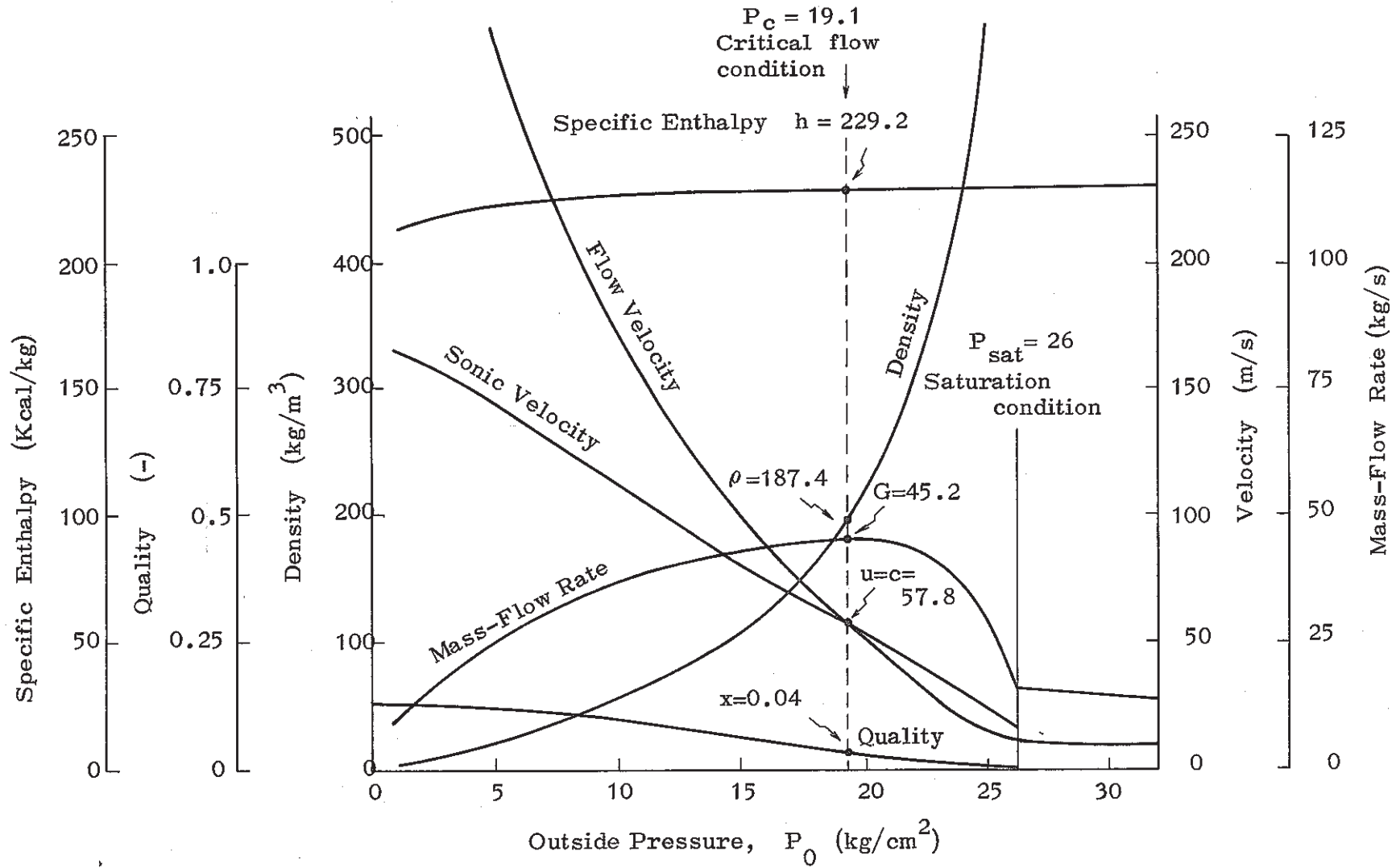


Fig. 2 Calculation Example of Initial Leak Rate for the Standard Problem Condition

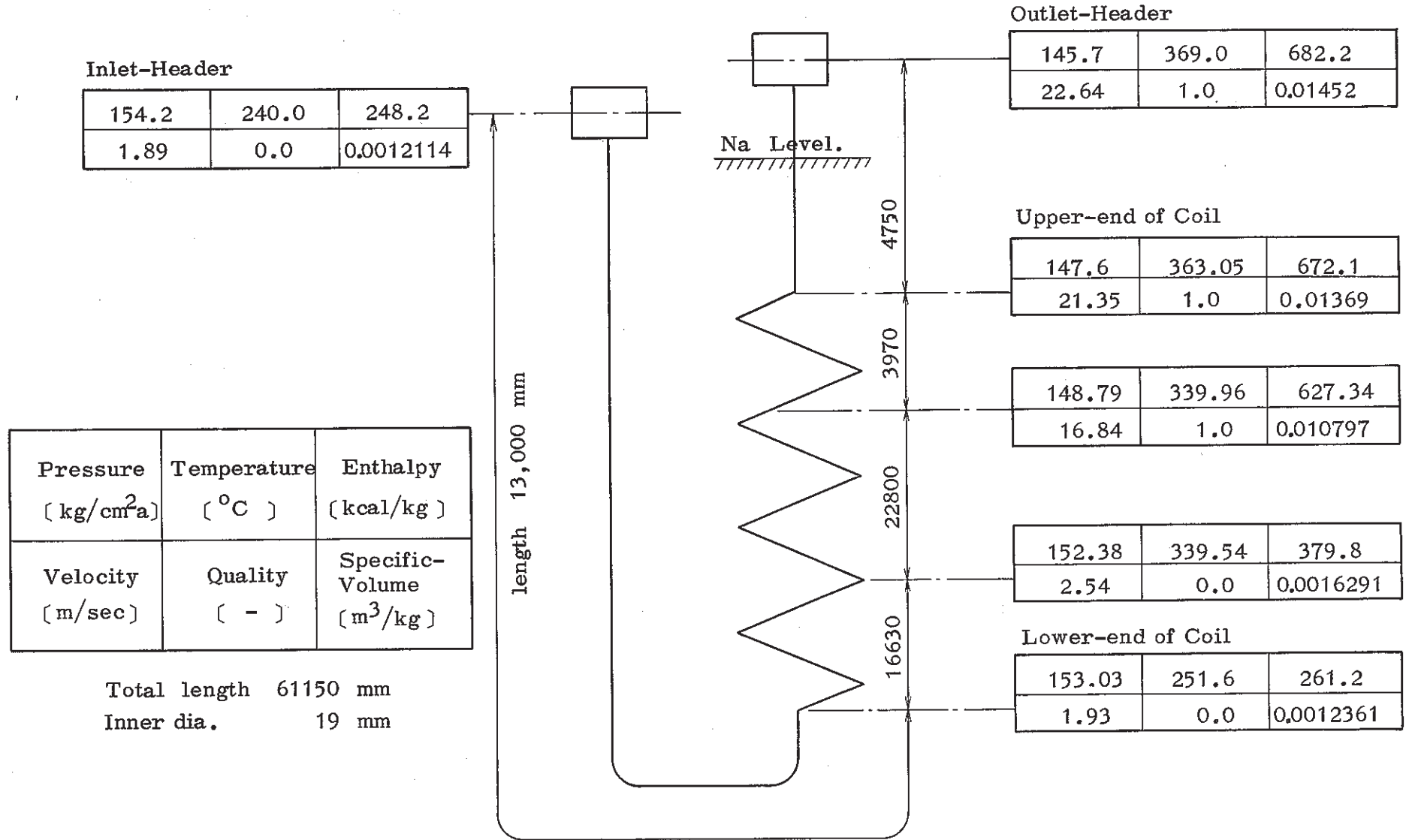


Fig. 3 Water/Steam Condition along Heat Transfer Tube of Helical Coil Type Steam Generator (Evaporator) of 200 MWt class.



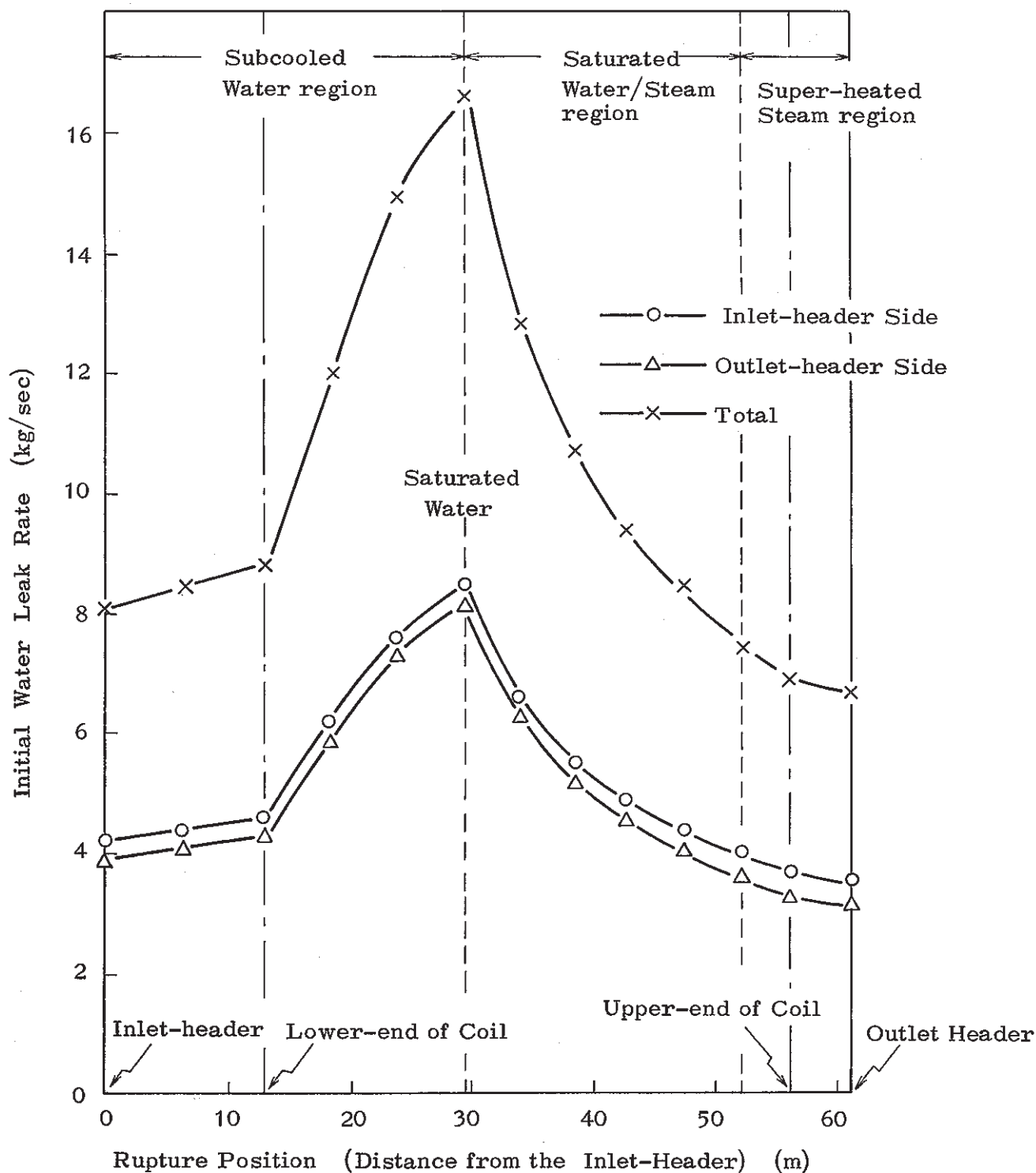


Fig. 4 Initial Water Leak Rate for 1 DEG Rupture of Helical-coil, Once-through Steam Generator

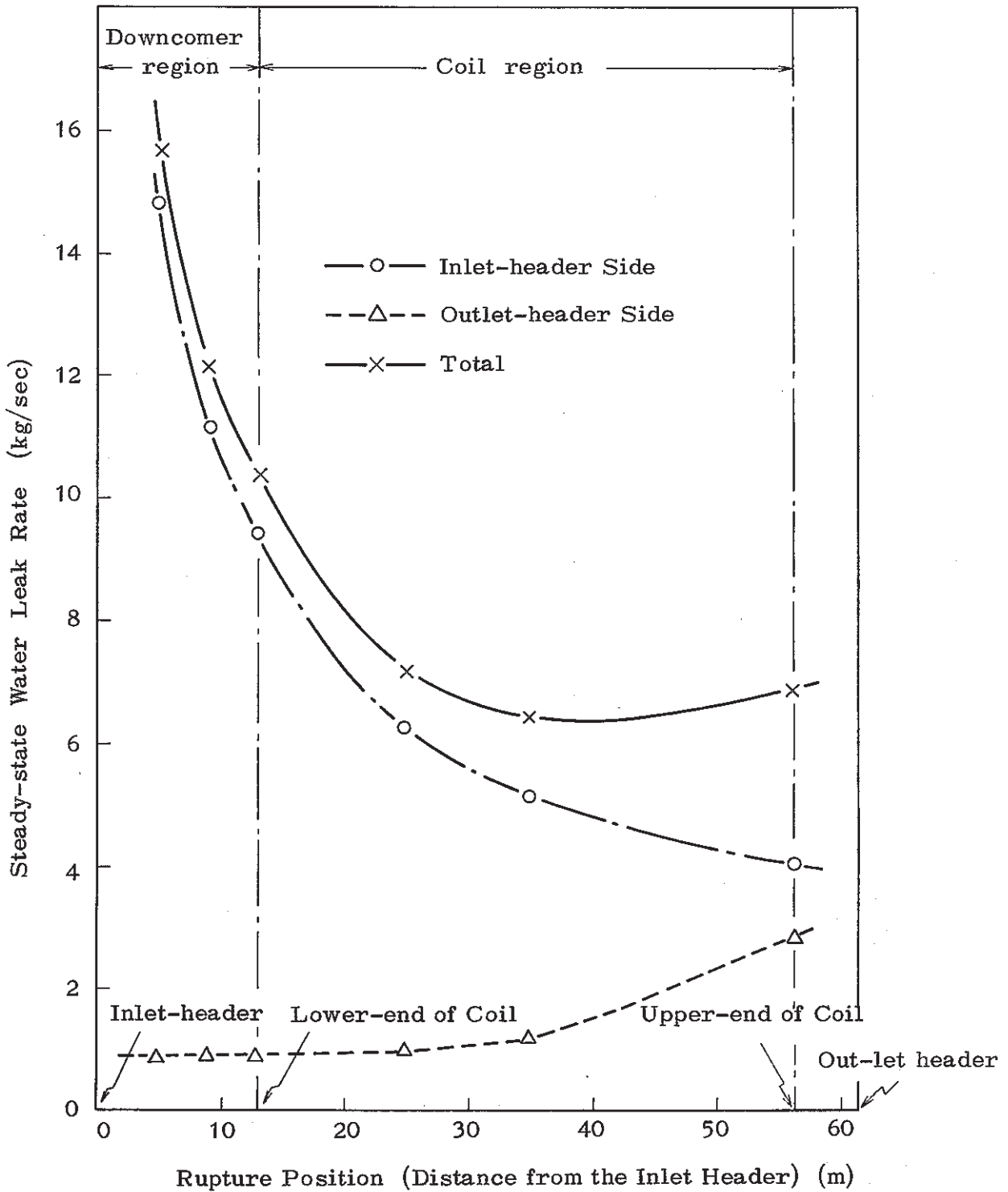


Fig. 5 Steady-state Water Leak Rate for 1 DEG Rupture of Helical-coil, Once-through Steam Generator.

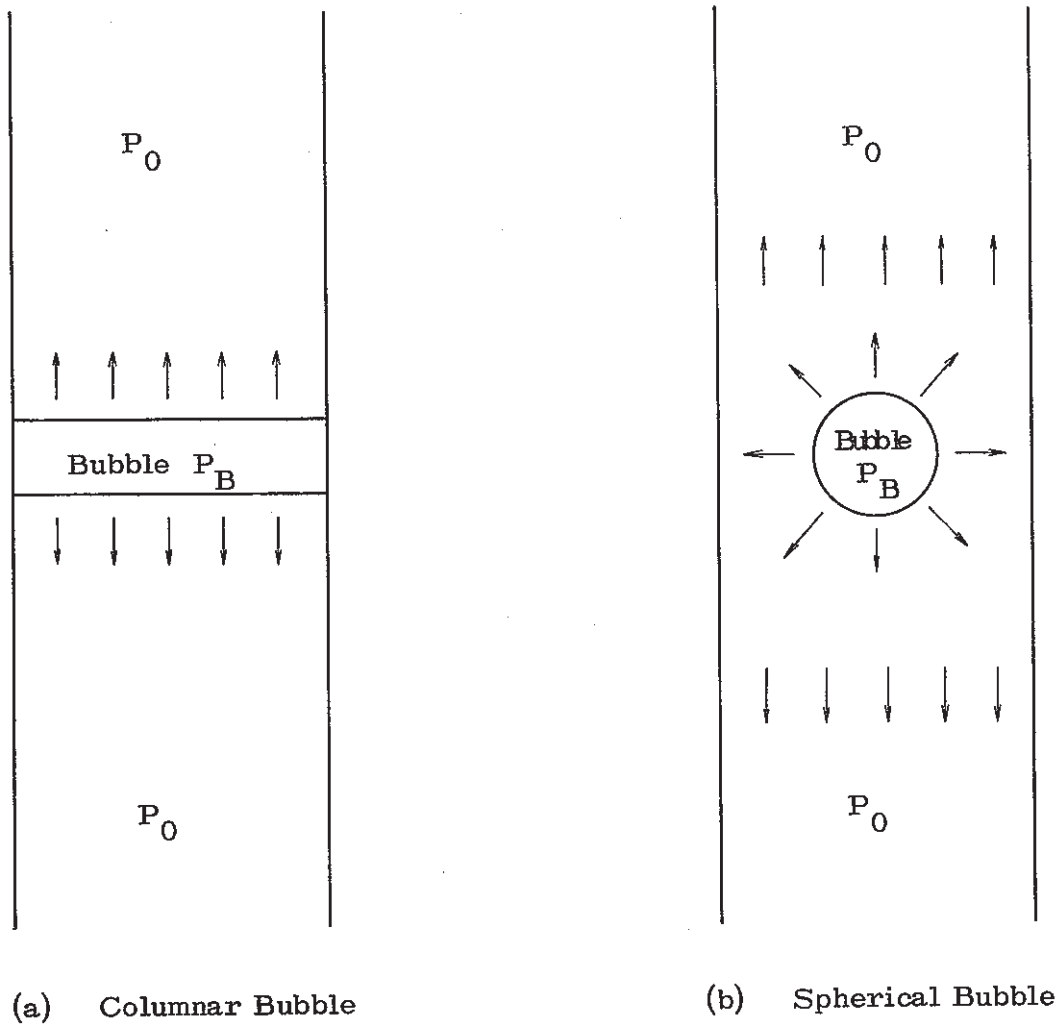


Fig. 6 One-dimensional Compressible Models

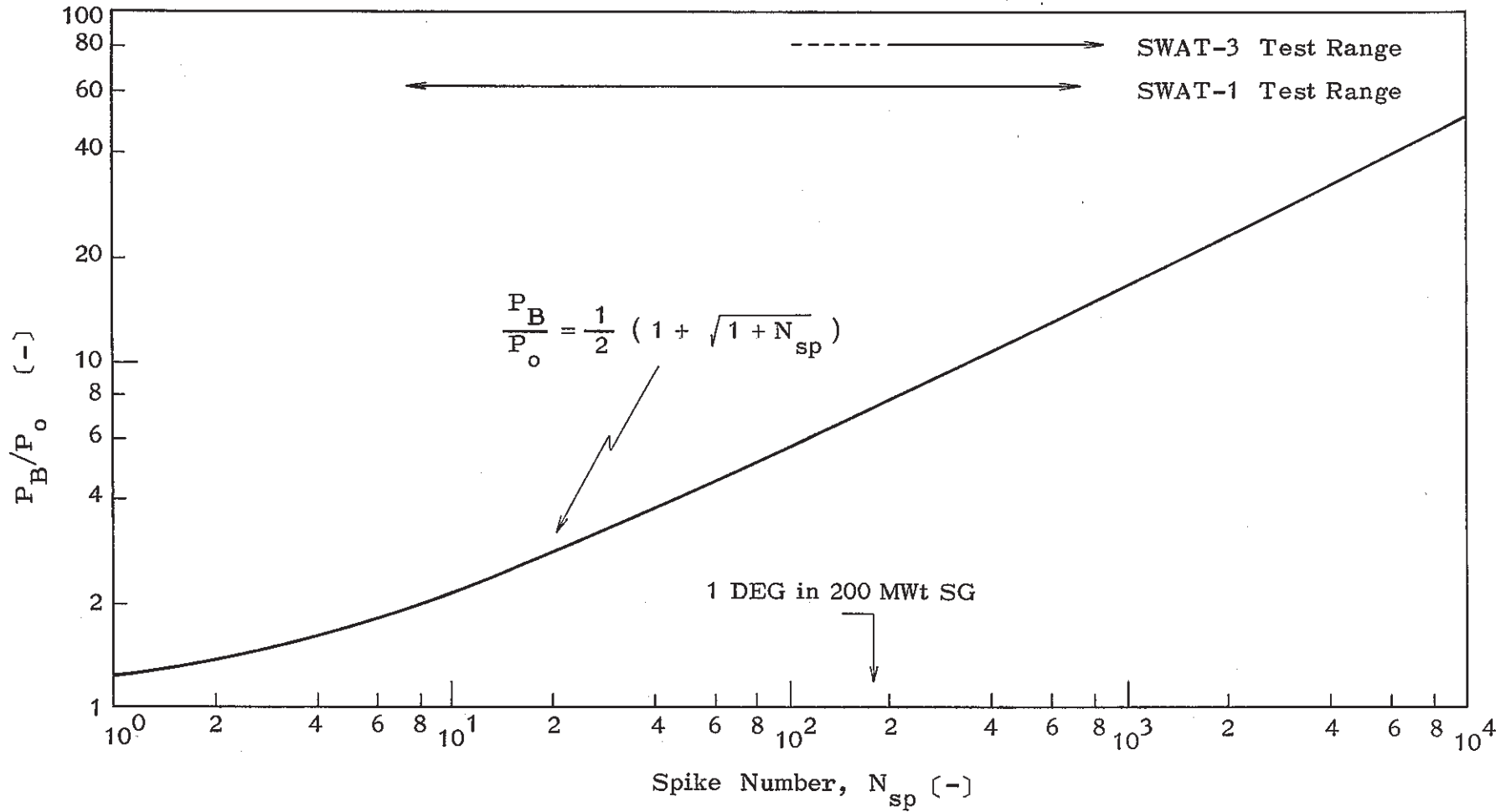


Fig. 7 Prediction of Spike Pressure by One-dimensional Compressible Model (Columnar Bubble Growth)

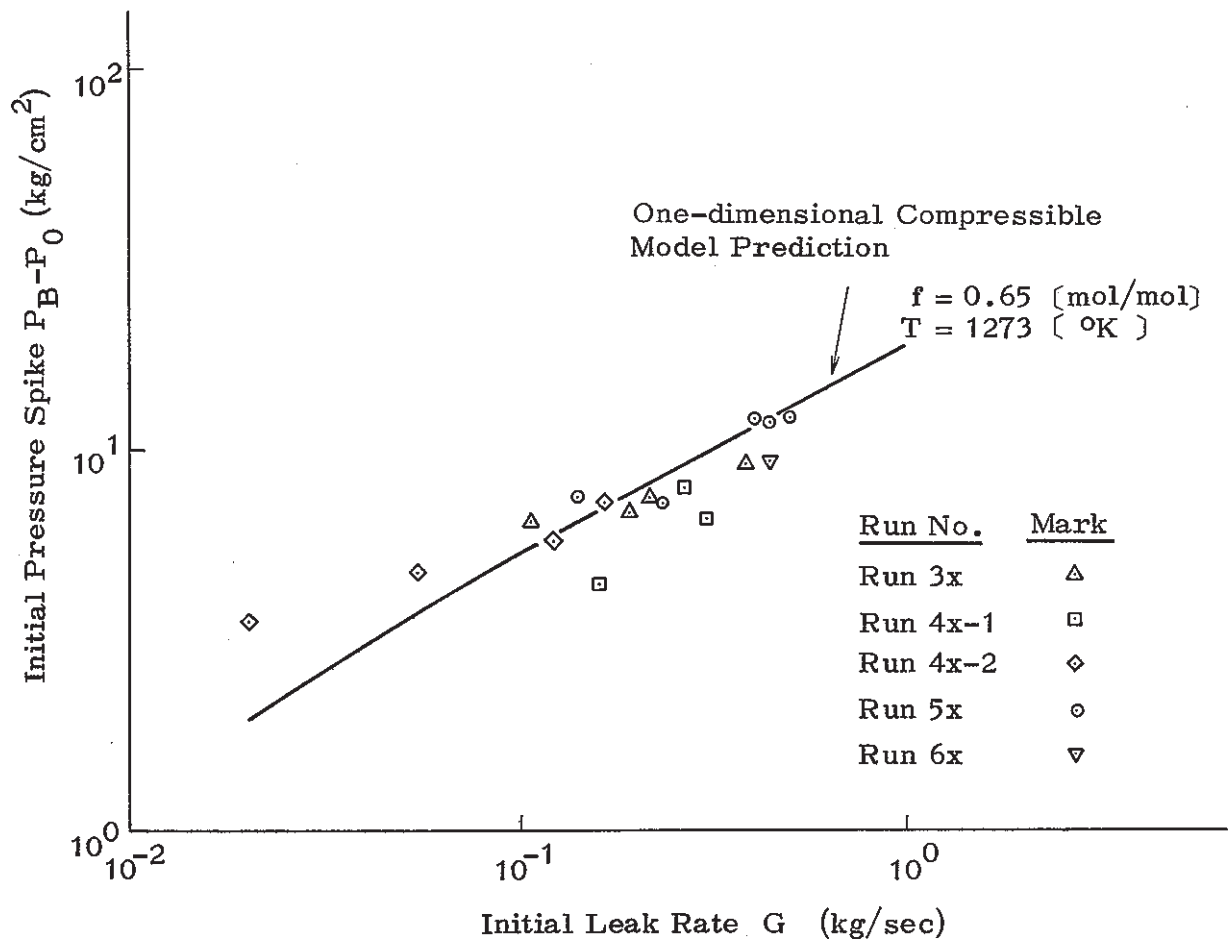


Fig. 8 Prediction of Initial Pressure Spike by Columnar Bubble, One-dimensional Compressible Model - Comparison with Experimental Data of SWAT-1 Tests (PNC)

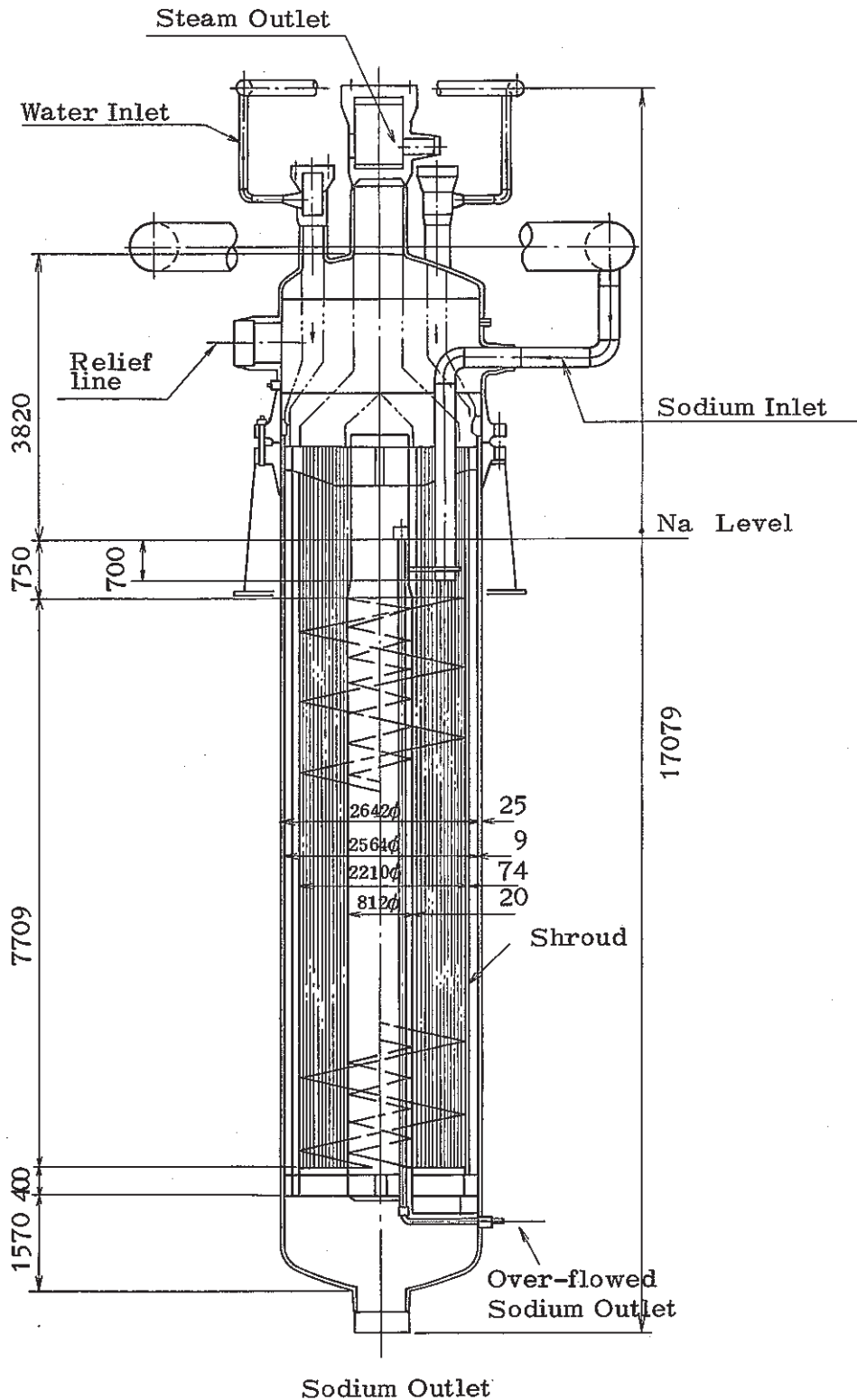


Fig. 9 Schematic Configuration of Helical Coil Type Steam Generator (Evaporator) of 200 MWt class

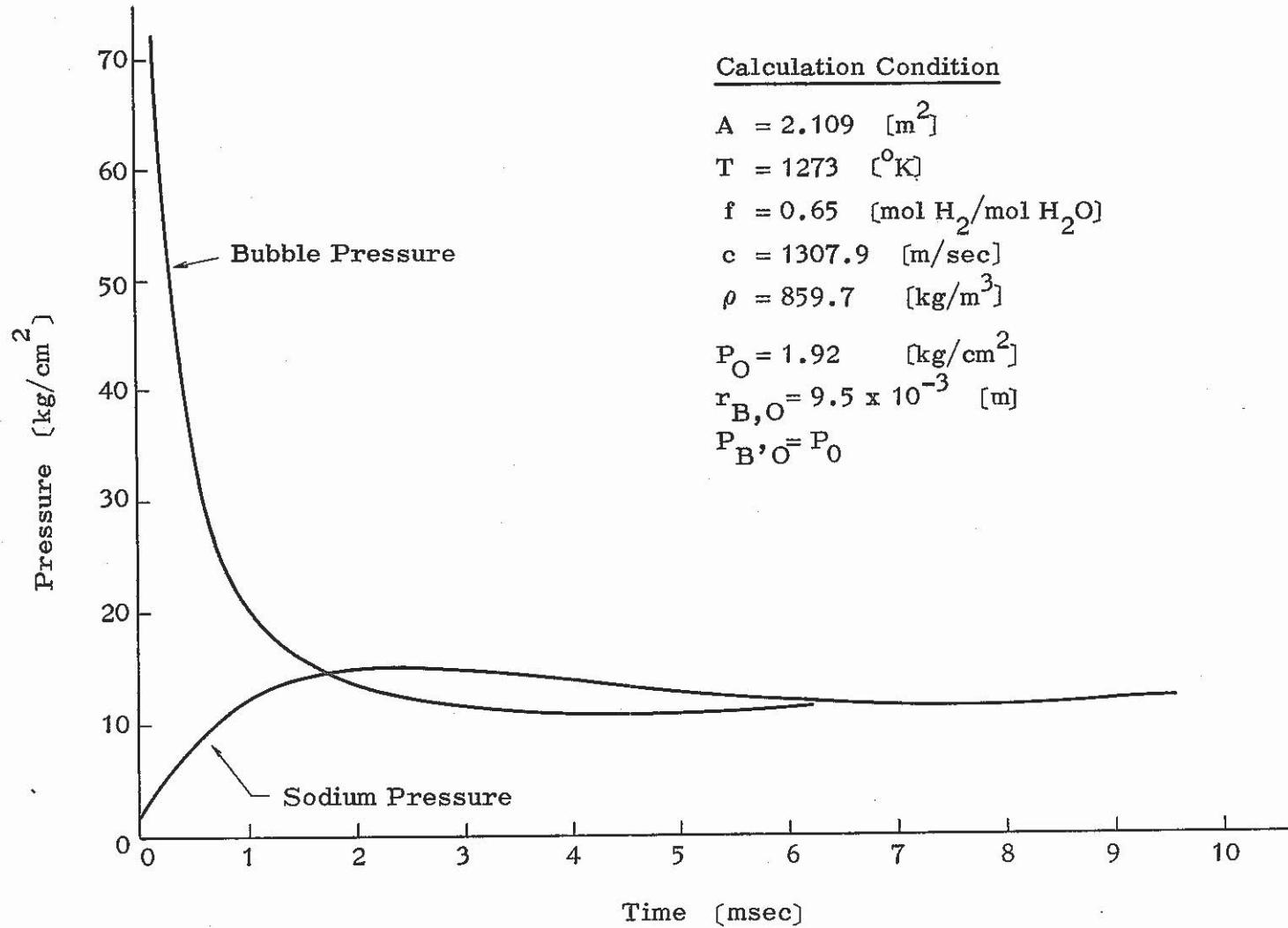


Fig. 10. Typical Pressure Transient of 1 DEG Rupture Calculated by Spherical Bubble One-dimensional Compressible Model (SP-AX Code)

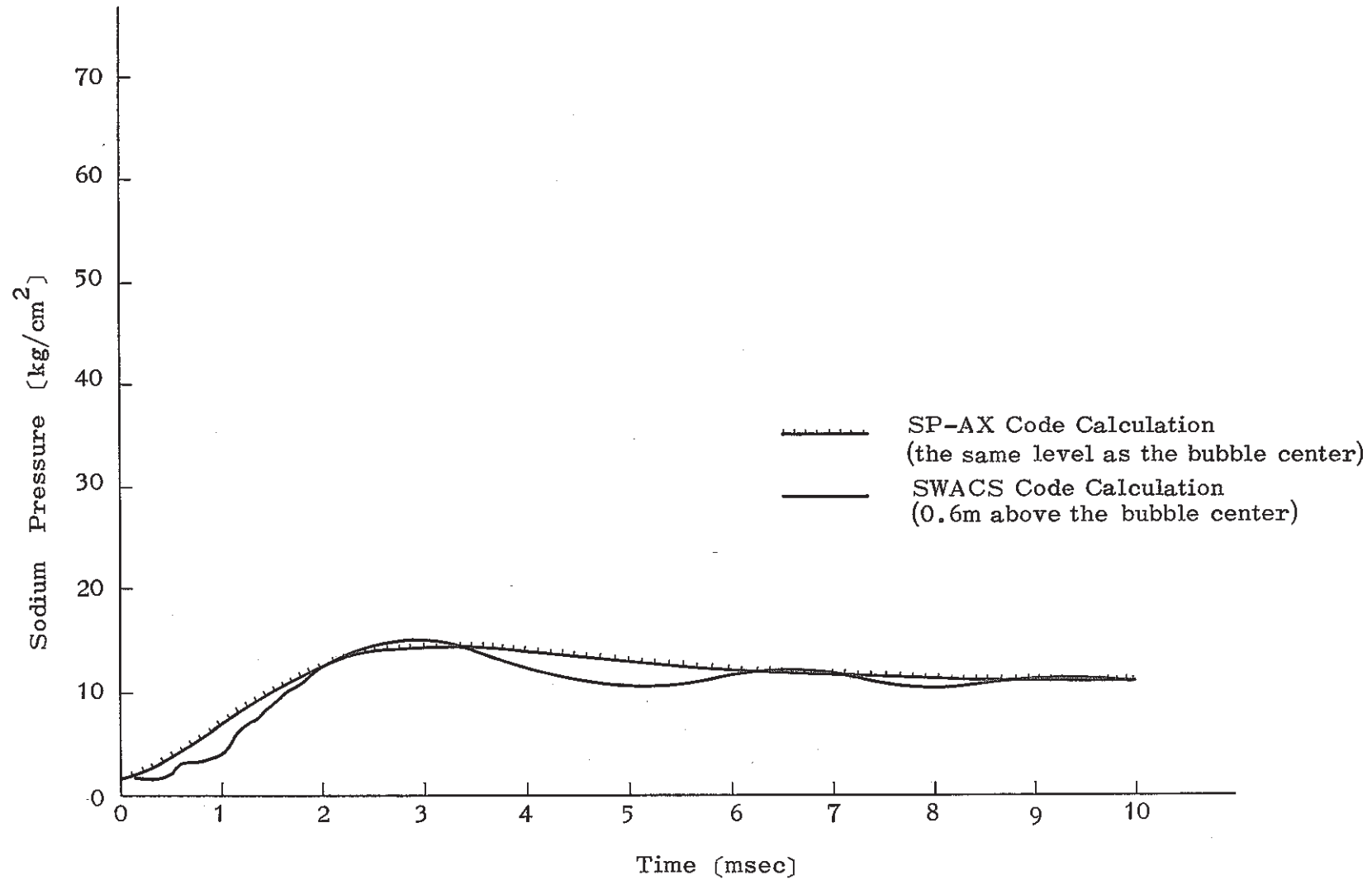


Fig. 11 Comparison of Spherical Compressible (SWACS) and Spherical Incompressible (SP-AX) Models.



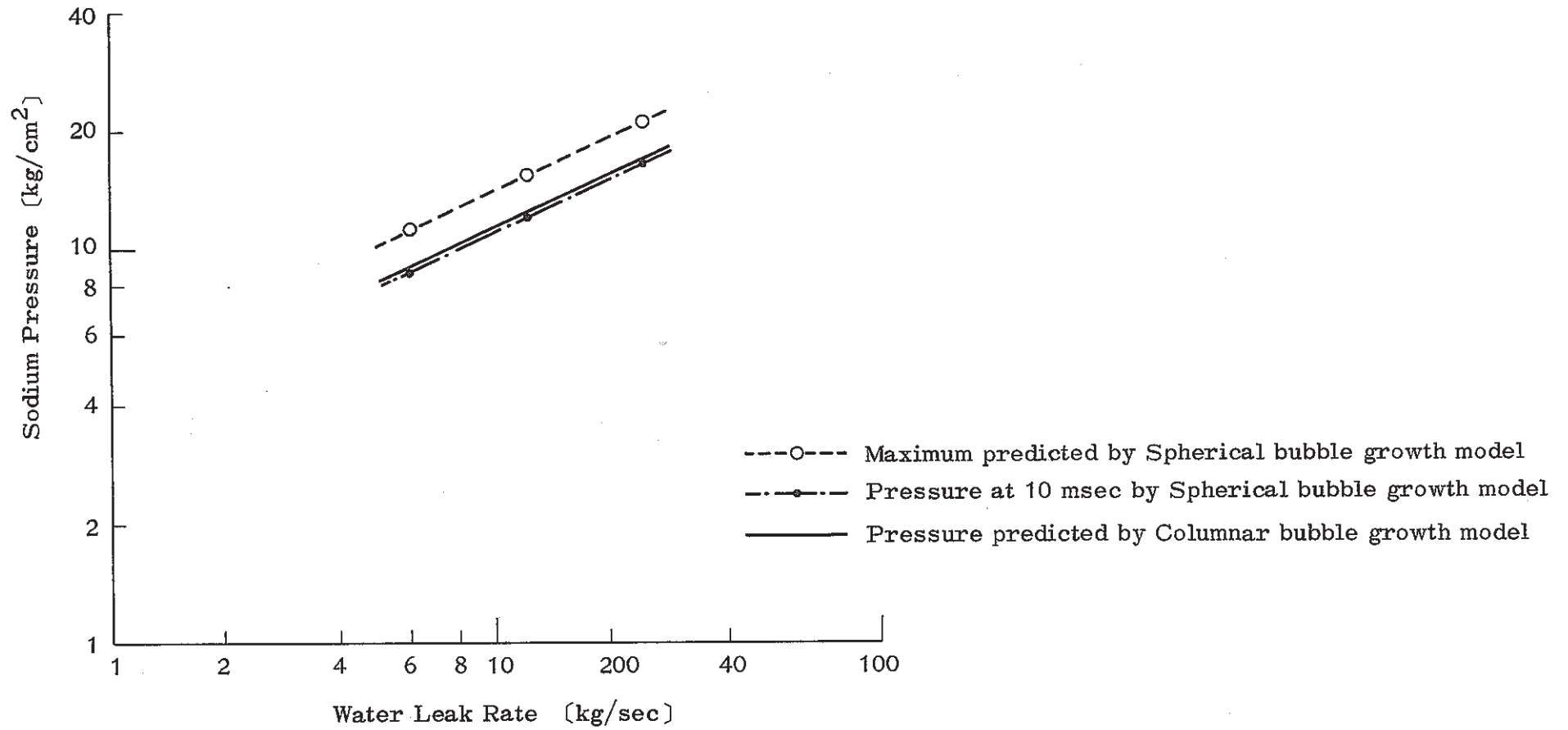


Fig. 12 Comparison of Columnar and Spherical Bubble Growth Models.

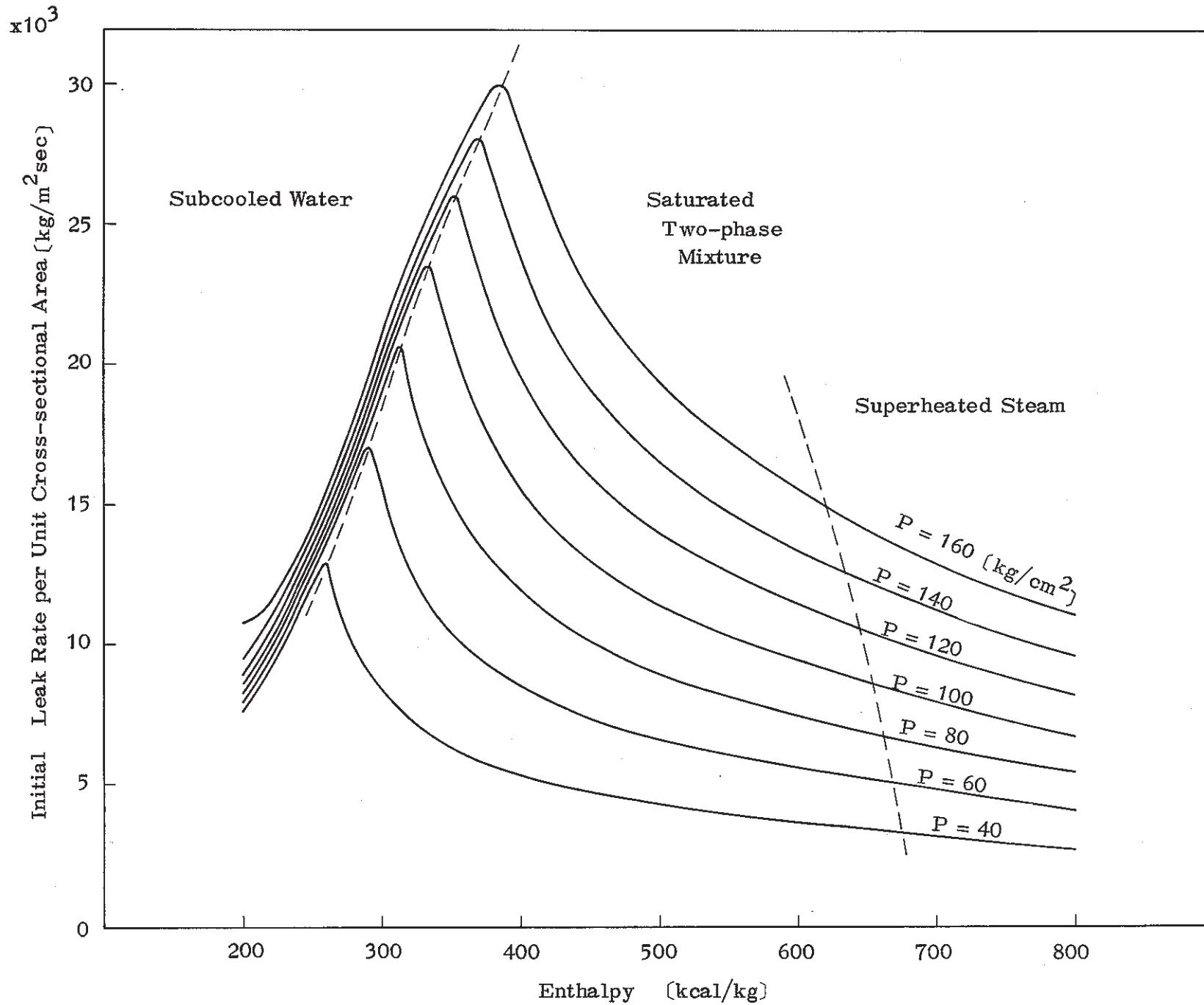


Fig. 13 Initial Leak Rate vs. Water/Steam Pressure and Enthalpy